




The role of atmospheric circulation patterns in driving recent changes in indices of extreme seasonal precipitation across Arctic Fennoscandia

Gareth J. Marshall¹  · Kirsti Jylhä² · Sonja Kivinen³ · Mikko Laapas² · Anita Verpe Dyrørdal⁴

Received: 18 June 2019 / Accepted: 20 May 2020 / Published online: 12 June 2020
© The Author(s) 2020

Abstract

Extreme precipitation events (EPEs) have a major impact across Arctic Fennoscandia (AF). Here we examine the spatial variability of seasonal 50-year trends in three EPEs across AF for 1968–2017, using daily precipitation data from 46 meteorological stations, and analyse how these are related to contemporaneous changes in the principal atmospheric circulation patterns that impact AF climate. Positive trends in seasonal wet-day precipitation (PRCPTOT) are widespread across AF in all seasons except autumn. Spring (autumn) has the most widespread negative (positive) trends in consecutive dry days (CDD). There is less seasonal dependence for trends in consecutive wet days (CWDs), but the majority of the stations show an increase. Clear seasonal differences in the circulation pattern that exerted most influence on these AF EPE trends exist. In spring, PRCPTOT and CDD are most affected by the Scandinavian pattern at more than half the stations while it also has a marked influence on CWD. The East Atlantic/Western Russia pattern generally has the greatest influence on the most station EPE trends in summer and autumn, yet has no effect during either spring or winter. In winter, the dominant circulation pattern across AF varies more between the different EPEs, with the North Atlantic Oscillation, Polar/Eurasia and East Atlantic patterns all exerting a major influence. There are distinct geographical distributions to the dominant pattern affecting particular EPEs in some seasons, especially winter, while in others there is no discernible spatial relationship.

Keywords Fennoscandia · Arctic · Precipitation · Extremes · Climate change · Atmospheric circulation pattern

Electronic supplementary material The online version of this article (<https://doi.org/10.1007/s10584-020-02747-w>) contains supplementary material, which is available to authorized users.

✉ Gareth J. Marshall
gjma@bas.ac.uk

Extended author information available on the last page of the article

1 Introduction

In recent decades, Arctic near-surface air temperatures (SATs) have warmed significantly faster than the global average and, since 1980, have increased more than twice that of the Northern Hemisphere average (Overland et al. 2016). In addition to this anthropogenically forced warming, human activity may be responsible for increased precipitation at northern high latitudes (Min et al. 2008). Indeed, observations and climate model simulations have demonstrated that Arctic precipitation increases in response to Arctic amplification (of SAT) (Anderson et al. 2018) and that both liquid and solid extreme precipitation events (hereinafter EPEs) intensify (O’Gorman 2014, 2015).

EPEs are one of the primary triggers of natural hazards in Arctic Fennoscandia (hereinafter AF), which comprises the northern areas of Norway, Sweden and Finland and the Kola Peninsula region of Russia (cf. Fig. 1), leading to avalanches, landslides and flooding (Jaedicke et al. 2008; Dyrørdal et al. 2012). In particular, heavy rainstorms or rain-on-snow events may lead to intense floods in Arctic catchments with low subsurface water storage because of permafrost or glacial cover (Dahlke et al. 2012; Nilsson et al. 2015). The importance of rainfall, rather than snowmelt, as a flood generating process has increased as regional temperatures have warmed and snow cover diminished (Vormoor et al. 2016). Resultant natural hazards, such as debris flow, can cause major disruption to local infrastructure (Beylich and Sandberg 2005; Callaghan et al. 2010). EPEs have also been cited as a major challenge for economic development in the Russian Arctic (Khlebnikova et al. 2018; Zolotokrylin et al. 2018).

EPEs can also have a marked impact on the natural environment, both directly, as organisms respond more to extremes than to averages, and, indirectly, through changes in carbon-cycle processes (e.g. Reichstein et al. 2013; Zwart et al. 2017). More directly, EPEs can affect plant productivity: heavy snowfall can break trunks or branches while heavy rainfall can flatten grasslands (Bjerke et al. 2014). The 2001 lemming population in the Abisko area of

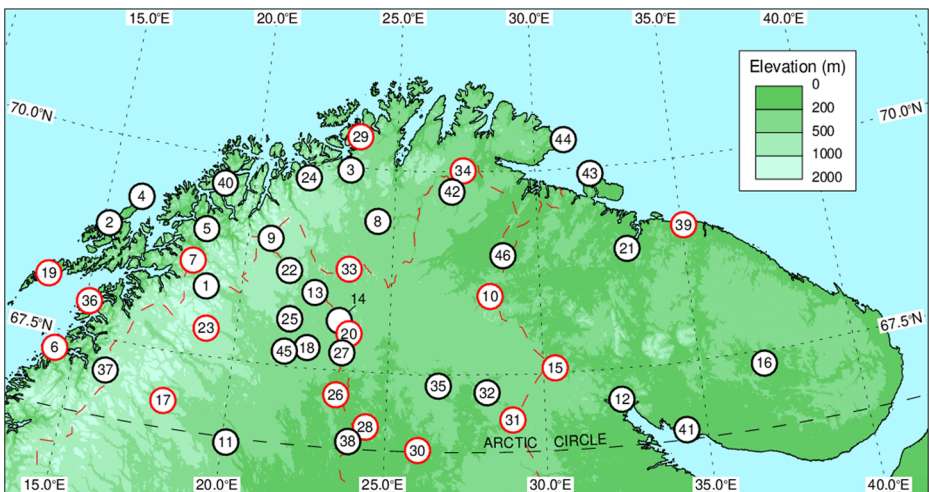


Fig. 1 Map showing locations of the 46 stations used in the analysis of extreme precipitation. The numbers are linked to the station names in Table 2. Stations with a red circle have potential inhomogeneities in their precipitation time series. International borders are shown as a dashed red line

northern Sweden plummeted when 150 mm of rain fell during 2 days followed by a marked drop in temperature and the formation of a 100-mm-thick pure ice layer in the snowpack (Callaghan et al. 2013). Similar impacts of ground ice on reindeer mortality have been reported (Hansen et al. 2014). EPEs during the nesting season can significantly impact the breeding success of birds (Yannic et al. 2014; Lamarre et al. 2018).

Inland convective storms (Achberger and Chen 2006) and intense sea-effect snowfall in coastal regions (Olsson et al. 2017) can generate significant EPEs in AF during summer and winter, respectively. Otherwise, regional EPEs are associated predominantly with weather fronts, often with high vertical velocities and moisture content (Hellström and Malmgren 2004; Hellström 2005; Mateeva et al. 2015), and extremely strong fronts have become more frequent in Europe (Schemm et al. 2017). However, over the Scandinavian Mountains, where the greatest regional snowfall extremes are simulated to occur (Räisänen 2016), there is also an orographic influence on EPEs (Dyrrdal et al. 2016). Modelling experiments indicate that precipitation at higher elevations responds more to changes in SAT (Sandvik et al. 2018); one contributing factor may be enhanced potential instability caused by high-elevation surface heating, leading to increased summer convective precipitation (Giorgi et al. 2016).

As the majority of AF EPEs are associated with weather fronts, their frequency is linked to macroscale atmospheric circulation (teleconnection) patterns that favour the passage of cyclonic fronts into the region. In particular, a positive North Atlantic Oscillation (NAO) leads to an increase in EPEs over AF in winter (Scaife et al. 2008; Willems 2013; Tabari and Willems 2018). Summer EPEs in Sweden have been linked to a well-developed ridge over western Russia (Hellström 2005). Similarly, the majority of days with EPEs in northwestern Russia (including the Kola Peninsula) have been characterised by low sea level pressure (SLP) to the north over the Barents Sea, whereby the inflow of colder air over the warmer land surface results in the intensification of convection (Mateeva et al. 2015). These descriptions match SLP anomalies associated with the East Atlantic/Western Russia (EAWR) and Scandinavian (SCA) patterns, respectively (Barnston and Livezey 1987). Together with the East Atlantic (EA) and Polar/Eurasia (POL) patterns, these are also the principal circulation patterns that control EPEs in northern Finland (Irannezhad et al. 2016, 2017).

The spatial and temporal distribution of precipitation varies markedly across AF. In northern Norway, mean annual precipitation ranges from 300 to 3000 mm (Førland et al. 2009). Moreover, the shape of the annual cycle is spatially uneven: the wettest seasons are autumn and winter in coastal AF, but inland summer has the greatest precipitation (Achberger and Chen 2006; Jylhä et al. 2010). Furthermore, the spatial structures of the annual and seasonal trends are complex, having greatly varying magnitude and sign within short distances (Achberger and Chen 2006; Marshall et al. 2018). Mean precipitation trends across AF generally show a wetting in recent decades, such as the increasing snowfall trend in Finnish Lapland (Luomaranta et al. 2019), but also with local areas of drying (Aalto et al. 2016; Marshall et al. 2016, 2018). Thus, there is a clear need to provide accurate information on how EPEs are changing in AF at a regional scale in order to support the planning of future infrastructure requirements to safeguard both human resources and the natural environment. Recent loss of winter sea ice in the Barents Sea to the north of AF has led to a greater proportion of ‘locally sourced’ moisture, which is likely to have impacted the regional precipitation regime (Kocev et al. 2016). Given that both the spatial distribution of precipitation across AF and the strength and pattern of some of the key atmospheric circulation patterns vary markedly across the calendar year, it is important to analyse changes in EPEs on a seasonal rather than annual basis.

Here, for the first time, we examine seasonal trends in three EPE indices over the past 50 years (1968–2017), using measured daily precipitation data from an array of meteorological stations across AF, and, in particular, determine the extent to which different circulation patterns are likely to be driving these seasonal changes. An additional motivation for this study is that it considers trends in EPE indices across the AF region as a whole, rather than in individual countries or as part of broad-scale global, European or Eurasian analyses as has been done previously. This allows us to better consider the spatial distribution of the seasonal EPE trends and their links to circulation patterns in the context of the regional geography.

The remainder of this paper is set out as follows: in Section 2, we describe the precipitation observations, how they were tested for temporal inhomogeneities and the other statistical methods used. We also define the three EPE indices examined and briefly describe the five atmospheric circulation patterns assessed as potential drivers of changes in regional EPEs. The analysis of the EPE trends themselves is provided in Online Resources 2, while in Section 3 we examine the potential influence of the circulation patterns on these trends. In Section 4, we compare our results with previous analyses and set them in the context of future regional projections of EPEs. Finally, in Section 5, we summarise our principal conclusions.

2 Data and methods

To calculate the EPE indices, we used daily precipitation data for the half century 1968–2017 from 46 stations across AF (Fig. 1 and Table 1). Station data rather than gridded reanalyses products were employed because the latter tend to markedly underestimate EPEs (Donat et al. 2014) and are relatively poor at getting even the regional annual precipitation trends correct (Marshall et al. 2018). One potential alternative is the gridded precipitation E-OBS dataset from the European Climate Assessment and Dataset (ECA&D), which is based on observations: unfortunately, in recent years, observations from relatively few Russian stations have been assimilated leading to missing data over the Kola Peninsula. The number of stations from each country in our analysis are as follows: Finland (9), Norway (17), Russia (8) and Sweden (12). The Finnish data were obtained from ECA&D, available at www.ecad.eu/dailydata/index.php (Klein Tank and Können 2003). Norwegian precipitation data were acquired from the Norwegian Meteorological Institute through their eKlima website, available via www.met.no/en/free-meteorological-data/Download-services. Data for the stations in the Kola Peninsula were obtained from the Russian Research Institute of Hydrometeorological Information World Data Centre (RIHMI-WDC) at www.aisori.meteo.ru/ClimateE. Swedish data were acquired from the Swedish Meteorological and Hydrological Institute (SMHI) website at www.smhi.se/klimatdata/meteorologi/ladda-ner-meteorologiska-observationer. The station number used in Fig. 1 and Table 1 is given in parentheses after the station name whenever it is discussed in the text.

We examined three different EPE indices: seasonal wet-day precipitation (PRCPTOT), maximum consecutive dry days (CDDs) and maximum consecutive wet days (CWDs). These are a subset of those proposed by the ETCCDI (Expert Team on Climate Change Detection and Indices) (Zhang et al. 2011) and are defined in Online Resources 1 (OR1). These three EPE indices were chosen as together they describe the total seasonal heavy precipitation and the duration of such events, which has a profound effect on their impact. Note that other EPEs, such as the simple daily intensity index, gave very similar results to PRCPTOT. We used standard Northern Hemisphere 3-month seasons: spring (March–April–May), summer (June–

Table 1 Station locations, elevation, and proportion of daily data for the 1968–2017 period

Station number in Fig. 1	Station name	WMO number	Latitude (°N)	Longitude (°E)	Elevation (m a.s.l.)	Proportion of available daily data (1968–2017)
1	Abisko	02022	68.36	18.82	388	98.5
2	Alsvåg i Vesterålen II	–	68.91	15.21	18	99.6
3	Alta Lufthavn	01049	69.98	23.36	3	93.7
4	Andøya	01010	69.31	16.13	10	98.0
5	Bardufoss	01023	69.06	18.54	76	99.4
6	Bodø VI	01152	67.27	14.36	13	99.9
7	Bones i Bardu	–	68.65	18.24	230	99.9
8	Cuovddatmohkki	01057	69.37	24.43	286	95.1
9	Enontekio Kilpisjärvi	02801	69.05	20.79	480	100.0
10	Inari Raja-Jooseppi Akujärvi	02818	68.47	28.32	185	99.5
11	Jokkmokk	02151	66.61	19.83	240	97.8
12	Kandalaksha	22,217	67.13	32.43	26	100.0
13	Karesuando	02080	68.44	22.45	331	100.0
14	Katkesuando	–	68.12	23.32	250	99.8
15	Kovdor	22,204	67.57	30.38	246	98.2
16	Krasnoshelye	22,235	67.35	37.05	155	97.2
17	Kvikkjokk Årrenjarka	02120	66.89	18.02	314	99.2
18	Lainio	02086	67.76	22.35	317	100.0
19	Leknes i Loføten	–	68.14	13.61	13	99.8
20	Muonio Alamuonio	02823	67.96	23.68	236	98.4
21	Murmansk	22,113	68.97	33.05	51	100.0
22	Naimakka	02060	68.68	21.53	403	99.5
23	Nikkaluokta	02036	67.85	19.02	470	92.1
24	Nordstrøm i Kvænangen	01045	69.84	21.89	6	99.2
25	Øvre Soppero	–	68.09	21.70	365	98.7
26	Pajala	02096	67.21	23.39	168	100.0
27	Parkajoki	–	67.73	23.49	205	99.9
28	Pello Konttajärvi	–	66.83	24.37	130	99.8
29	Porsa II	–	70.40	23.63	38	98.2
30	Rovaniemi Apukka	02813	66.58	26.01	106	100.0
31	Salla Kelloselkä	–	66.94	28.98	200	99.4
32	Savukoski KK	02815	67.29	28.18	180	99.8
33	Šihččajávri	01199	68.76	23.54	382	99.4
34	Sirbma	–	70.02	27.40	51	97.9
35	Sodankylä Arctic Research Centre (ARC)	02836	67.37	26.63	179	100.0
36	Steigen	–	67.92	15.11	28,31	99.8
37	Sulitjelma	–	67.13	16.07	142	99.7
38	Svanstein	–	66.65	23.86	80	96.8
39	Teriberka	22,028	69.18	35.08	30	96.5
40	Tromsø	01026	69.65	18.94	100	99.9
41	Umba	22,324	66.68	34.35	39	97.5
42	Utšjoki Kevo	02805	69.76	27.01	107	100.0
43	Vaida Guba	22,003	69.93	31.98	8	97.8
44	Vardø Radio	01098	70.37	31.10	10	99.9
45	Vittangi	–	67.69	21.63	250	99.0
46	Yaniskoski	22,101	68.97	28.78	98	94.8

July–August), autumn (September–October–November) and winter (December–January–February).

We note that there are several difficulties in obtaining reliable precipitation measurements in the Arctic. Blowing snow may give ‘additional’ precipitation: when there is only blowing snow, it can be excluded through data quality control but during instances of combined precipitation and blowing snow, it is difficult to discriminate (Førland et al. 2009). Conversely, harsh weather conditions can mean significant undercatches in standard precipitation gauges, particularly for solid precipitation (e.g. Kochendorfer et al. 2017). Thus, increases in the proportion of liquid precipitation in a warmer Arctic may lead to potentially fictitious positive trends in precipitation (Førland et al. 2009). Unfortunately, correction factors are not simple to apply as they vary according to wind speed, temperature, precipitation type (solid, frozen or mixed) and gauge type (Groisman et al. 2014). An additional consideration is the openness of a station to various wind directions, which is usually unknown as a function of time. Therefore, such corrections are not made routinely by meteorological agencies.

There is also the possibility for precipitation time series to be affected by non-climatic inhomogeneities—modifications to observational instruments and practices, relocations and changes in the station environment. To detect such potential inhomogeneities, we used the HOMER software (Mestre et al. 2013), which has been utilised in a previous study of climate data from AF (Kivinen et al. 2017). The detection is based on a comparison with available neighbouring ‘reference’ stations. Given the sporadic nature of daily precipitation and its small correlation radius (Groisman et al. 2005), the scheme uses annual data for initial comparison, as the higher correlations allow HOMER to detect much smaller inhomogeneities.

Using HOMER, we found that 17 of the 46 time series examined had apparent inhomogeneities and these stations are discriminated in Fig. 1. Where possible, we compared the statistical breaks in the data to station metadata. In some cases, there was a potential reason for the inhomogeneity: for example, a break in 1980 in the Sirbma (34) precipitation time series may be associated with a concurrent 60-m move. Nonetheless, there were a number of inhomogeneities found by HOMER where available station metadata offer no apparent potential cause for the statistical breaks so they are likely to be either a natural occurrence or caused by an undocumented change at the station. Therefore, as we cannot prove that any particular inhomogeneity is definitively non-climatic, we have included results from all 46 stations in our analysis. However, we focus our analysis on regional changes experienced by several stations and flag individual results based on potentially inhomogeneous time series if relevant.

EPE trends were only calculated when 47 out of the 50 years (94%) of data were available. Previous sensitivity experiments revealed that unbiased estimates of CDD and CWD durations required records with less than 10% of missing values (Zolina et al. 2010), so we assumed that a maximum of 6% missing data should not markedly bias our findings. Stations were chosen on the basis they had enough data to calculate EPE trends for at least one season.

We calculated the 50-year trends in EPEs using ordinary least squares (OLS) regression techniques while using the non-parametric Mann-Kendall test to calculate trend significance (Alexander and Arblaster 2008; Łupikasza 2017). The latter test is widely used for evaluating the presence of monotonic trends and makes no assumption for normality, only that the data are temporally independent, so is appropriate for the EPE data. As OLS can be sensitive to outliers, we also calculated the magnitude of the trends using (the non-parametric) ‘Sen’s slope method’ (Sen 1968). The results were generally very similar so we used the original OLS trends.

The principal goal of this paper is to determine whether the observed trends in EPEs may be linked to changes in atmospheric circulation patterns. We utilised monthly data for indices of

the North Atlantic Oscillation (NAO), East Atlantic (EA), East Atlantic/Western Russia (EAWR), Scandinavia (SCA) and Polar/Eurasia (POL) patterns. The data were obtained from the Climate Prediction Centre at www.cpc.ncep.noaa.gov/data/teledoc/telecontents.shtml, where there are also details of the pressure anomalies associated with the different patterns (see also Irannezhad et al. (2017) for a brief description). Many of these circulation patterns were first derived statistically by Barnston and Livezey (1987), using Empirical Orthogonal Function (EOF) analysis, and have since been shown to exert significant control on regional climate variability across much of Europe. Seasonal indices were simply calculated as the mean of the three monthly values. We used the non-parametric Spearman's rank correlation to determine whether there was a statistically significant relationship between detrended time series of EPEs and circulation pattern indices. To determine the pattern with the greatest influence on EPE changes at a station over the past 50 years, we calculated the magnitude of the seasonal trend of each pattern index (Table 3) multiplied by the regression coefficient between the pattern and the station's EPE time series. We note that while this calculation does not necessarily imply cause and effect, it does signify the likely relative influence of the different circulation patterns on an EPE index at a station.

3 Results

3.1 Seasonal trends in the EPE indices

Due to space constraints, the full description of the seasonal EPE trends is provided in Online Resources 2, including box-whisker plots of the data distribution for each EPE index across the seasons (Fig. OR2.4) and maps displaying the spatial distribution of the stations with significant trends displayed in Figs. OR2.5 to OR2.7. The principal findings can be summarised as follows.

We find that positive trends in PRCPTOT for 1968–2017 were widespread across AF in all seasons bar autumn, with more than 40% of stations examined having a significant trend ($p < 0.10$) in these three seasons (Table 2, Fig. OR2.5). In spring, greater than half the stations had a significant positive trend, including those along the Norwegian coast whereas in summer and winter significant trends were generally limited to inland areas of AF, indicating a seasonally varying role for the regional orography in controlling PRCPTOT trends. Although the two EPEs are not directly related, given that autumn had the fewest positive trends in PRCPTOT, it is unsurprising that it had the most widespread positive trends in CDD (Table 2, Fig. OR2.6). In the other three seasons, the clear majority of AF stations had negative trends in CDD, with spring having the greatest proportion (~ half), located especially in the north and west of the region. The majority of stations showed an increase in CWD but there were generally fewer with significant trends than for the two other EPEs examined (Table 2, Fig. OR2.7) No clear inverse relationship between changes in CDD and CWD was detected.

3.2 Influence of atmospheric circulation patterns on EPE indices

In Figs. 2, 3, and 4, we show which atmospheric circulation pattern likely made the greatest contribution (as defined earlier in the methodology) to driving observed EPE changes at the AF stations for the 1968–2017 period differentiated by EPE and season. We distinguish stations where the circulation pattern was likely to have driven the trend in EPE: that is, (i)

Table 2 Summary of EPE trends at AF stations

Index/season	No. of stations	Stations with pos. trend (%)	Stations with sig. pos. trend (%)	Stations with neg. trend (%)	Stations with sig. neg. trend (%)
PRCPTOT					
Spring	43	84.8	56.5	15.2	0.0
Summer	40	73.9	39.1	26.1	0.0
Autumn	43	45.7	2.2	54.3	4.3
Winter	41	82.6	41.3	17.4	0.0
CDD					
Spring	43	8.7	0.0	91.3	45.7
Summer	40	28.3	2.2	71.7	17.4
Autumn	43	71.7	17.4	28.3	2.2
Winter	41	34.8	2.2	65.2	10.9
CWD					
Spring	43	58.7	17.4	41.3	2.2
Summer	40	50.0	13.0	50.0	6.5
Autumn	43	63.0	10.9	37.0	2.2
Winter	41	60.9	15.2	39.1	2.2

a statistically significant correlation between the detrended time series of the EPE and the dominant circulation pattern index existed and (ii) the latter had a significant seasonal trend (Table 3) that, given the sign of the correlation, would force the EPE in the same direction as the observed trend. We also discriminate between stations where only (i), (ii) or neither is true. Box-whisker plots showing the distribution of the correlations between each EPE and circulation pattern by season for the AF stations are given in Fig OR3.1.

3.2.1 PRCPTOT (seasonal total wet-day precipitation)

In spring, the SCA was clearly the dominant circulation pattern affecting PRCPTOT in AF, with more than 75% of stations revealing this pattern to have had the greatest influence in this season (Fig. 2a). There was a significant negative trend in spring SCA (Table 3), which, in combination with the negative correlation between SCA and PRCPTOT at most stations (Fig. OR3.1j), meant that changes in this circulation pattern drove increased PRCPTOT at the majority of AF stations (stations represented by yellow squares). The majority of other stations had the EA as the dominant pattern, which actually had a larger but positive trend in spring than SCA (Table 3).

During summer and autumn (Fig. 2b, c), the most frequent dominant pattern was the EAWR, which had significant negative trends in both these seasons (Table 3). Correlations between EAWR and PRCPTOT in summer and autumn were generally negative, with slightly more stations having a positive correlation in autumn (Fig. OR3.1g). Therefore, the negative EAWR trend contributed to the significant positive PRCPTOT trends in summer detected at many inland stations (cf. Fig. OR2.5b and red squares in Fig. 2b). Conversely, despite a statistically significant EAWR trend in autumn (Table 3), there were no widespread significant changes in PRCPTOT in this season (cf. Table 2, Figs. OR2.5c and 2c).

In winter, two circulation patterns had the greatest impact on PRCPTOT: the NAO and the POL were the dominant pattern at 54% and 34% of stations, respectively (Fig. 2d). There was a distinct geographical pattern to where these two patterns were dominant across AF. The

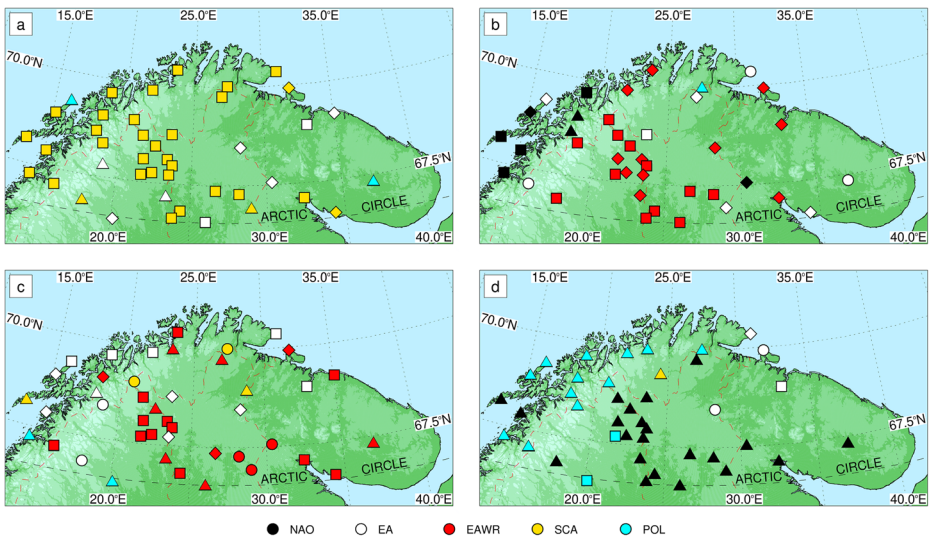


Fig. 2 Spatial distribution of the most influential circulation pattern on seasonal trends in PRCPTOT for 1968–2017: (a) spring, (b) summer, (c) autumn, and (d) winter. Stations where there was both (i) a statistically significant correlation between the detrended time series of PRCPTOT and the dominant circulation pattern index and (ii) the latter had a significant seasonal trend that, given the sign of the correlation, would force PRCPTOT in the same direction as the observed trends are shown as a square; those stations where only (i) was true are shown as a triangle; those stations where only (ii) was true are shown as a diamond, and those stations where neither (i) nor (ii) was true are shown as a circle

greater influence of POL was generally prevalent in the north and west, along the Norwegian coast and in the Scandinavian Mountains. Correlations between POL and station PRCPTOT were positive in these regions (and indeed at most AF stations, cf. Fig. OR3.1m) and thus the negative trend in POL (Table 3) actually worked against the weak positive trends in PRCPTOT observed there (hence blue triangles rather than squares in Fig. 2d). The NAO predominated across much of the remainder of AF, but its positive winter trend during the study period was not statistically significant (Table 3) (thus black triangles instead of squares).

3.2.2 CDD

The SCA had the greatest influence on CDD trends (at 60% of stations) in spring (Fig. 3a). At all of these stations (yellow squares), there was a statistically significant positive correlation

Table 3 Fifty-year seasonal trends (1968–2017) of atmospheric circulation patterns together with 95% confidence intervals. Units are per decade. Trends marked with an asterisk are statistically significant (all at $p < 0.01$)

Teleconnection	Season			
Pattern	Spring	Summer	Autumn	Winter
NAO	+0.06 ± 0.12	−0.24 ± 0.14*	−0.02 ± 0.13	+0.17 ± 0.21
EA	+0.21 ± 0.10*	+0.38 ± 0.12*	+0.20 ± 0.14*	+0.22 ± 0.15*
EAWR	+0.01 ± 0.11	−0.32 ± 0.13*	−0.20 ± 0.12*	−0.01 ± 0.15
SCA	−0.18 ± 0.10*	−0.20 ± 0.12*	+0.08 ± 0.12	−0.06 ± 0.13
POL	−0.15 ± 0.10*	+0.08 ± 0.12	−0.11 ± 0.16	−0.18 ± 0.13*

between CDD and SCA (Fig. OR3.1k), so the negative trend in this pattern (Table 3) was consistent with the observed widespread negative trends in CDD (Table 2, Fig. OR2.5a). Besides the SCA, two other circulation patterns were also prominent in spring: EA and POL were most influential at 26% and 14% of stations, respectively (Fig. 3a). With one exception in the Kola Peninsula, the stations dominated by POL were situated on the west coast of Norway and all had a significant negative trend in CDD. However, POL did not show a trend that would have forced CDD in the observed direction. Instead, the correlation between POL and CDD at many of these stations was negative (Fig. OR3.1n), which, in combination with the significant negative trend in spring POL (Table 3), suggests that changes in POL would have driven an increase rather than decrease in CDD (blue triangles).

In summer and autumn, the EAWR was the predominant governing circulation pattern. The spatial distribution of the stations for which this pattern had the greatest influence on CDD in summer was similar to the equivalent example for PRCPTOT (cf. Figs. 2b and 3b). However, in autumn, the situation was somewhat different, with the majority of the western coastal stations having EAWR rather than EA as the most influential pattern. Another seasonal difference from PRCPTOT was the greater proportion of stations with SCA as the dominant pattern in autumn (cf. Figs. 2c and 3c), which had no significant trend in this season (Table 3). The majority of those stations that had significant increases in CDD in autumn (Fig. OR2.6c) had EAWR as the greatest contributing pattern. However, although there was a significant negative trend in autumn EAWR (Table 3), there were very few stations where this pattern was significantly correlated with CDD (Fig. OR3.1h, relatively few red squares in Fig. 3c): Sulitjlema (39) was the only station with such a relationship and a significant CDD increase.

The spatial extent of the impact of the NAO on winter CDD across AF was reduced compared to PRCPTOT. Instead, both POL (39%) and EA (32%) had the most influence on CDD at a greater proportion of stations (Fig. 3d). CDD was not governed by the NAO at any of the Norwegian stations studied, but otherwise there was less of a clear spatial pattern in the primary circulation pattern affecting CDD trends in winter than for the other two EPEs examined. The correlations between the circulation patterns and CDD at the few stations with

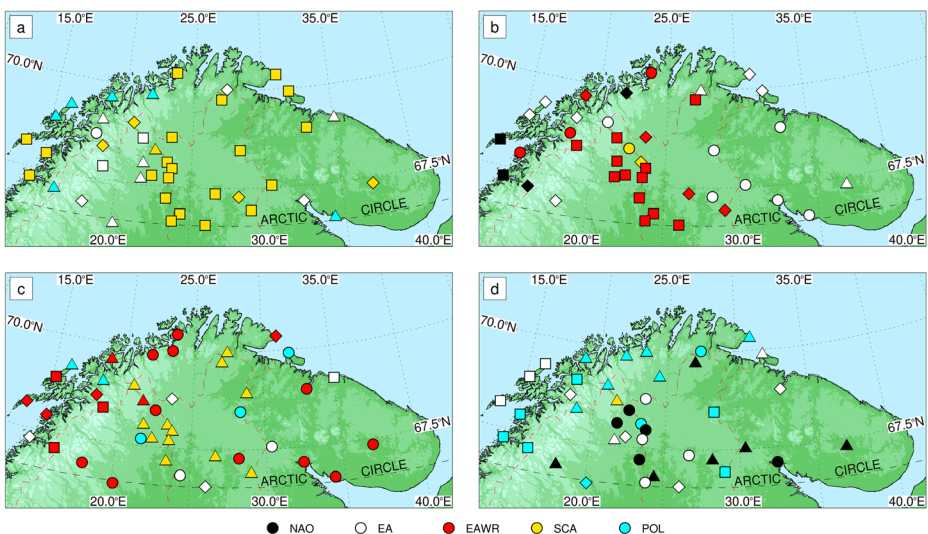


Fig. 3 As Fig. 2 but for CDD

significant trends in winter CDD were such that it is unlikely that any of them had a marked influence (cf. Figs. OR2.6d and 3d).

3.2.3 CWD

The principal circulation patterns that governed AF trends in spring CWD were the same as those for CDD: the SCA (44%), EA (26%) and POL (23%). Nonetheless, the geographical pattern of greatest influence associated with each was different. For example, those stations where SCA had the most impact on CWD trends were predominantly located in the north and west of AF, including the Scandinavian Mountains, whereas those where it most influenced CDD tended to be further inland, to the east (cf. Figs. 3a and 4a). Conversely, the stations where POL was dominant on CWD trends were primarily in the south of the region as compared to the west coast for CDD changes. The negative correlation between SCA and CWD at the Norwegian coastal stations in spring (Fig. OR3.11) in combination with the significant negative winter trend in this pattern (Table 3) indicates that SCA variability was likely to have been a contributing factor to the significant positive trends in CWD observed at some of these stations (cf. Fig. OR2.7a and yellow squares in Fig. 4a).

In summer, the geographical distribution of the influential circulation patterns was rather scattered. EA, rather than EAWR, was the pattern governing CWD trends at the greatest number of stations (40%) with such stations distributed across most of AF (Fig. 4b). The negative correlation between EA and CWD at Andøya (4) and Bardufoss (5) together with the very large positive summer trend in this pattern (Table 3) was therefore possibly responsible for the significant negative trends in summer CWD at these two stations (cf. Fig. OR2.7b and white squares in Fig. 4b). For autumn, similar to the other two EPEs in this study, EAWR was the most common dominant pattern affecting CWD in autumn (Fig. 4c) but, despite having a widespread influence across AF, this pattern had significant correlations with CWD at relatively few AF stations (red squares in Fig. 4c) and none at the small number of stations having a significant seasonal trend in CWD (Fig. OR2.7c).

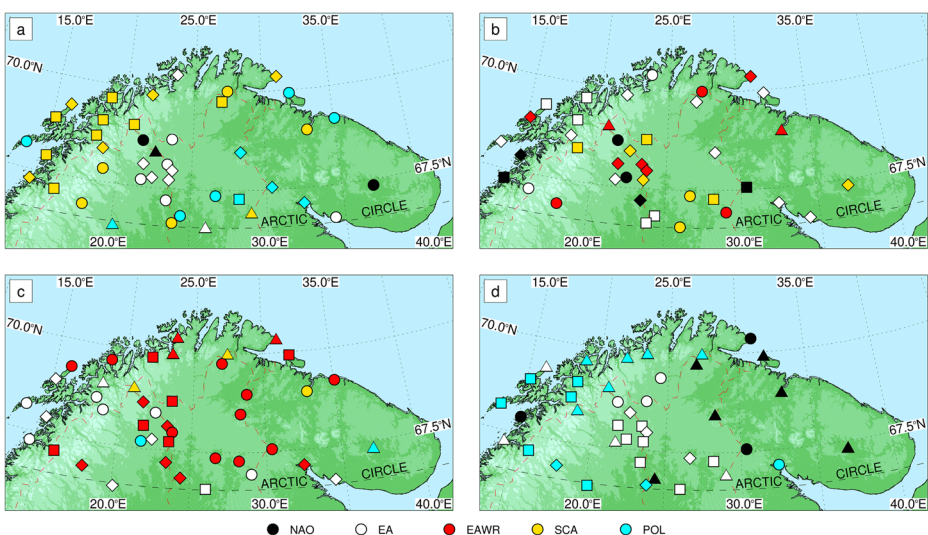


Fig. 4 As Fig. 2 but for CWD

EA was the pattern that had the primary influence on CWD changes at the most AF stations in winter (41%), followed by POL (37%) and NAO (22%). The geographical distribution of where these three patterns were dominant across AF was relatively well defined (Fig. 4d). POL had most impact at western stations and those in the south-west, NAO had the greatest effect at stations in the east while EA governed the CWD trends in the central region of northern Sweden and Finland. The positive correlations between EA and CWD in many of these ‘central’ stations meant that the significant positive trend in this circulation pattern may well have contributed to the significant trends observed at some of these stations, such as Katkesuando (14) and Lainio (18) (cf. Fig. OR2.7d and white squares in Fig. 4d).

4 Discussion

Here we set our principal findings in the context of previous work and future climate projections. Based on our study, more than 40% of stations examined across AF had significant ($p < 0.10$) positive trends in PRCPTOT in all seasons bar autumn. However, the spatial distribution of such stations varied between seasons, suggesting a seasonally changing importance to the control that the regional orography exerts on PRCPTOT trends, likely to do with concomitant changes in the strength and direction of the regional wind field. Previous studies also demonstrated an increasing trend in annual PRCPTOT across the region based on observations (Klein Tank and Können 2003; Moberg et al. 2006) and gridded data (Irannezhad et al. 2017). Casaneuva et al. (2014) examined seasonal trends in total precipitation (RR) for Europe from 1950 to 2010 based on the E-OBS dataset, including the southern part of AF as defined here. Their results differed slightly from ours, in that widespread positive trends occurred in autumn as well as other seasons, perhaps as a consequence of the differing time periods examined.

Our results indicate that CDD had a significant negative trend at about 50% (25%) of AF stations in spring (summer) and a significant increase at about 20% of stations in autumn. A significant positive trend in CWD was detected at almost 20% of stations in spring. Preceding studies described a small decrease in annual CDD across AF throughout the twentieth century (Frich et al. 2002; Alexander et al. 2006; Donat et al. 2013). A mix of trends in both CDD and CWD occurred in northern Norway and Sweden during 1961–2004 (Achberger and Chen 2006) and northern Finland for 1961–2011 (Irannezhad et al. 2017) and, in agreement with this study, there was a predominance of negative (positive) trends for CDD (CWD). However, two earlier studies (Zolina et al. 2013; Casaneuva et al. 2014) revealed that the largest negative (positive) trends in CDD (CWD) happened during winter, primarily in the western half of AF. There is no evidence of these spatial and temporal patterns in the present study: in the case of Zolina et al. (2013), the discrepancy may be because of differing study periods and season definition.

Analysis of which atmospheric circulation pattern had the greatest influence on the 50-year changes in the three EPEs across AF demonstrated clear seasonal differences. In spring, SCA was the dominant teleconnection mode at more than half the stations examined for both PRCPTOT and CDD, while also having a marked influence on CWD trends across parts of AF (Figs. 2a, 3a and 4a). A positive SCA has a primary positive centre of action (above average SLP) over eastern Fennoscandia, and the resultant anticyclonic circulation causes anomalous southerly flow and reduced precipitation over AF (e.g. Bueh and Nakamura 2007; Liu et al. 2014). Moreover, Popova (2007) reported that a positive SCA was associated with negative

snow depth anomalies in AF. However, as the 50-year seasonal trend in spring SCA was strongly negative (Table 3), this led to an intensification of cyclonic activity and greater precipitation over AF, as revealed by the widespread significant increases in PRCPTOT and decreases in CDD in spring (Figs. OR2.5a and OR2.6a). Irannezhad et al. (2017) also showed that SCA was the circulation index that had the highest correlation with annual CDD in northern Finland. The EA and POL patterns exerted the greatest influence over a quarter of AF stations for one or more of the EPE trends in spring. There was a distinct geographical distribution to the dominant pattern impacting spring CWD changes in AF.

The EAWR pattern generally had the most influence on AF EPE trends in both summer and autumn, but not so during spring and winter (Figs. 2, 3, and 4). As significant correlations existed between EAWR and the EPEs across all seasons in AF, this seasonal distinction was primarily because of the significant (negligible) trends in the summer and autumn (spring and winter) EAWR indices (Table 3). For example, we note that Casanueva et al. (2014) found that correlations between EAWR and EPEs in AF were actually much stronger in winter than in autumn while Irannezhad et al. (2017) demonstrated that EAWR was the circulation pattern with the highest correlation to annual PRCPTOT in northern Finland. A positive EAWR has been linked to anomalous northerly flow over the Barents Sea with markedly increased precipitation over AF in winter (e.g. Ionita 2014; Lim 2015). However, we find that in summer, the relationship between EAWR and PRCPTOT was predominantly negative and hence the significant negative trend in EAWR contributed to the increasing PRCPTOT trends observed across AF in this season (Fig. 2b). The EA actually had the largest impact on the summer CWD trend at the most stations and the marked seasonal increase in this index may have been responsible for driving the significant negative trends in parts of northern Norway (Figs. OR2.7b and 4b). In autumn, EAWR was the circulation pattern with the greatest influence on the most AF stations for all three EPEs studied. Nevertheless, both the EA and SCA patterns were also dominant at more than 25% of AF stations for one or more of the EPE trends in this season (Figs. 2c, 3, and 4c).

In winter, there was more variation between the different EPE trends as to which was the dominant circulation pattern in AF. For PRCPTOT, the NAO was the primary driver at over half the stations (Fig. 2d). This circulation pattern plays a major role in driving climate variability across much of Europe (e.g. Hurrell et al. 2003; Bader et al. 2011). In its positive phase, the NAO is associated with below-normal SLP in the north-east Atlantic, leading to anomalously southwesterly flow over AF, bringing warmer, moist air from the south that gives enhanced regional precipitation. For example, Marshall et al. (2016) showed that the NAO explained about half of the interannual winter precipitation variability in the Kola Peninsula. Although not statistically significant, the magnitude of the 1968–2017 winter NAO trend was still markedly positive (Table 3), indicating it was likely to have driven the significant positive trends in PRCPTOT observed in central AF (cf. Fig. OR2.5d). POL was the dominant pattern affecting the most winter CDD trends across AF. Its positive phase is associated with enhanced onshore northerly flow over AF and positive regional snow-depth anomalies (Popova 2007). Moreover, across Norway, it was the dominant mode of circulation variability affecting trends for all three EPEs. However, there were few significant winter EPE trends in this region. The EA was the pattern most affecting CWD changes at most AF stations (Fig. 4d). It is likely that this trend would have contributed to the significant CWD trends observed at some stations in northern Sweden and Finland (Figs. OR2.7d and 4d): this spatial pattern is also seen in the correlation coefficients between EA and CWD in Fig. 3 of Casanueva et al. (2014). We note that there were also examples of significant trends in EPEs that appear independent of the

broad-scale circulation, perhaps indicative of changing precipitation intensity from small-scale convection events.

Given the significant rise in SAT across AF for the study period, it is not surprising that our findings correspond with future climate projections, which indicate that EPEs are likely to become more frequent and widespread in the Arctic as SAT increases further. Although there are reported regional exceptions (Ye 2018), the generally close relationship between EPEs and SAT is evident in studies examining the difference in EPEs between 1.5 and 2.0 °C warming scenarios. These show significant intensification of EPEs in the AF region at a mean global temperature only 0.5 °C higher (e.g. King and Karoly 2017; Aeronson et al. 2018; Barcikowska et al. 2018), associated with a greater poleward shift of the midlatitude stormtrack and intensely precipitating extratropical cyclones (Hawcroft et al. 2018). Thus, the geographical extent of statistically significant trends in EPEs shown in the present study is likely to become more widespread across the AF region in the future.

Indeed, analyses using an ensemble of models generally show increases in the regional EPE indices (e.g. Saha et al. 2006; Kharin et al. 2013; Chen et al. 2014; Lehtonen et al. 2014; Benestad et al. 2016; Hanssen-Bauer et al. 2017). An examination of the CMIP5 models (e.g. Taylor et al. 2012) for different Representative Concentration Pathway (RCP) scenarios indicated significant increases in PRCPTOT over AF for 2081–2100 relative to 1981–2000, increasing in magnitude with emissions (Sillmann et al. 2013). However, such projections vary significantly between models in Scandinavia (Screen et al. 2015) and there are marked differences in uncertainty ranges in EPE projections over Europe between global and regional models (Lehtonen et al. 2014). Thus, in order to provide the most beneficial information for socio-economic planning, it is important that future work focuses on analysing model uncertainty. Comparing recent trends in the models with those derived from observations, as described here, is an important component of such analyses. Furthermore, for the models to provide accurate projections, it is essential that they correctly reproduce the varying seasonal relationships between the primary atmospheric circulation patterns and EPEs as revealed by our study (Fig. OR3.1): future work will focus on the ability of the current CMIP6 models to accomplish this.

5 Conclusions

In this study, we calculated seasonal 50-year trends in three extreme precipitation events (EPEs) across Arctic Fennoscandia (AF) and analysed how these related to concurrent changes in the principal atmospheric circulation patterns affecting the region.

The main results of the study are as follows:

- More than 40% of stations examined had significant ($p < 0.10$) positive trends in seasonal wet-day precipitation (PRCPTOT) in all seasons bar autumn.
- Consecutive dry days (CDDs) had a significant negative trend at about 50% (20%) of the stations in spring (summer) and a significant positive trends at about 20% of the stations in autumn.
- A significant positive trend in CWD was detected at almost 20% of the stations in spring and winter.
- Decreases in SCA in spring and in EAWR in summer likely contributed to the observed increases in PRCPTPT and CWD and decreases in CDD in those seasons.

- Relatively few statistically significant trends in EPEs were detected in autumn, and the influence of the circulation patterns on them remained less clear than in the other seasons.
- Increases in PRCPTPT in inland areas in winter were most commonly linked to NAO and those in CWD to EA, although the lack of a statistically significant linear positive trend in NAO prevents a firm conclusion.

A need exists to provide information on how EPEs are changing in order to support the planning of future infrastructure requirements. Based on climate model projections, it is possible to assess if and how rapidly the geographical extent of statistically significant trends in EPEs shown in the present study will become more widespread across AF in the future. While our observational results generally correspond with climate projections available in the literature, our study also demonstrates that local variability necessitates that a large number of stations are required in order to obtain a reliable estimate of the regional-scale changes to date.

Acknowledgements G.J.M was supported by the Russian-British project ‘Multiplatform remote sensing of the impact of climate change on northern forests of Russia’ funded by the British Council (grant no. 352397111) and the Ministry of Science and Higher Education of the Russian Federation (project RFMEFI61618X0099). S.K. was funded by the Academy of Finland Strategic Research Council project IBC-Carbon (312559). Dr. Heikki Tuomenvirta is acknowledged for discussions.

Open Access This article is licensed under a Creative Commons Attribution 4.0 International License, which permits use, sharing, adaptation, distribution and reproduction in any medium or format, as long as you give appropriate credit to the original author(s) and the source, provide a link to the Creative Commons licence, and indicate if changes were made. The images or other third party material in this article are included in the article's Creative Commons licence, unless indicated otherwise in a credit line to the material. If material is not included in the article's Creative Commons licence and your intended use is not permitted by statutory regulation or exceeds the permitted use, you will need to obtain permission directly from the copyright holder. To view a copy of this licence, visit <http://creativecommons.org/licenses/by/4.0/>.

References

- Aalto J, Pirinen P, Jylhä K (2016) New gridded daily climatology of Finland: permutation-based uncertainty estimates and temporal trends in climate. *J Geophys Res Atmos* 121:3807–3823. <https://doi.org/10.1002/2015JD024651>
- Achberger C, Chen D (2006) Trend of extreme precipitation in Sweden and Norway during 1961–2004. Res rep C72 ISSN 1400-383X, Earth Sciences Centre, Göteborg University, Göteborg, 58 pp
- Aerenson T, Tebaldi C, Sanderson B, Lamarque J-F (2018) Changes in a suite of indicators of extreme temperature and precipitation under 1.5 and 2 degrees warming. *Environ Res Lett* 13:035009. <https://doi.org/10.1088/1748-9326/aaafd6>
- Alexander LV, Arblaster JM (2008) Assessing trends in observed and modelled climate extremes over Australia in relation to future projections. *Int J Climatol* 29:417–435. <https://doi.org/10.1002/joc.1730>
- Alexander LV et al (2006) Global observed changes in daily extremes of temperature and precipitation. *J Geophys Res* 111:D05109. <https://doi.org/10.1029/2005JD006290>
- Anderson BT, Feldl N, Lintner BR (2018) Emergent behavior of Arctic precipitation in response to enhanced Arctic warming. *J Geophys Res Atmos* 123:2704–2717. <https://doi.org/10.1002/2017JD026799>
- Bader J, Mesquita MDS, Hodges KI, Keenlyside N, Østerhus S, Miles M (2011) A review on Northern Hemisphere sea-ice, storminess and the North Atlantic Oscillation: observations and projected changes. *Atmos Res* 101:809–834. <https://doi.org/10.1016/j.atmosres.2011.04.007>
- Barcikowska MJ, Weaver SJ, Feser F, Russo S, Schenk F, Stone DA, Wehner MF, Zahn M (2018) Euro-Atlantic winter storminess and precipitation extremes under 1.5°C vs. 2°C warming scenarios. *Earth Syst Dyn* 9:679–699. <https://doi.org/10.5194/esd-9-679-2018>

- Barnston AG, Livezey RE (1987) Classification, seasonality and persistence of low-frequency atmospheric circulation patterns. *Mon Weather Rev* 115:1083–1126. [https://doi.org/10.1175/1520-0493\(1987\)115<1083:CSAPOL>2.0.CO;2](https://doi.org/10.1175/1520-0493(1987)115<1083:CSAPOL>2.0.CO;2)
- Benestad RE, Parding KM, Isaksen K, Mezghani A (2016) Climate change and projections for the Barents region: what is expected to change and what will stay the same? *Environ Res Lett* 11:054017. <https://doi.org/10.1088/1748-9326/11/5/054017>
- Beylich AA, Sandberg O (2005) Geomorphic effects of the extreme rainfall event of 20–21 July, 2004 in the Latnjavagge catchment, northern Swedish Lapland. *Geogr Ann Ser A Phys Geog* 87:409–419. <https://doi.org/10.1111/j.0435-3676.2005.00267.x>
- Bjerke JW, Karlsen SR, Høgda KA, Maines E, Jepsen JU, Lovibond S, Vikhamar-Schuler D, Tømmervik H (2014) Record-low primary productivity and high plant damage in the Nordic Arctic region in 2012 caused by multiple weather events and pest outbreaks. *Environ Res Lett* 9:084006. <https://doi.org/10.1088/1748-9326/9/8/084006>
- Bueh C, Nakamura H (2007) Scandinavian pattern and its climatic impact. *Q J Roy Met Soc* 133:2117–2131. <https://doi.org/10.1002/qj.173>
- Callaghan TV, Bergholm F, Christensen TR, Jonasson C, Kokfelt U, Johansson M (2010) A new climate era in the sub-Arctic: accelerating climate changes and multiple impacts. *Geophys Res Lett* 37:L14705. <https://doi.org/10.1029/2009GL042064>
- Callaghan TV et al (2013) Ecosystem change and stability over multiple decades in the Swedish subarctic: complex processes and multiple drivers. *Phil Trans Roy Soc B* 368:20120488. <https://doi.org/10.1098/rstb.2012.0488>
- Casanueva A, Rodríguez-Puebla C, Frías MD, González-Reviriego N (2014) Variability of extreme precipitation over Europe and its relationships with teleconnection patterns. *Hydrol Earth Syst Sci* 18:709–725. <https://doi.org/10.5194/hess-18-709-2014>
- Chen D, Achberger C, Ou T, Postgård U, Walther A, Liao Y (2014) Projecting future local precipitation and its extremes for Sweden. *Geogr Ann Ser A Phys Geog* 97:25–39. <https://doi.org/10.1111/geoa.12084>
- Dahlke HE, Lyon SW, Stedinger JR, Rosqvist G, Jansson P (2012) Contrasting trends in floods for two sub-arctic catchments in northern Sweden – does glacier presence matter? *Hydrol Earth Syst Sci* 16:2123–2141. <https://doi.org/10.5194/hess-16-2123-2012>
- Donat MG et al (2013) Updated analyses of temperature and precipitation extreme indices since the beginning of the twentieth century: the HadEX2 dataset. *J Geophys Res Atmos* 118:2098–2118. <https://doi.org/10.1002/jgrd.50150>
- Donat MG, Sillmann J, Wild S, Alexander LV, Lippmann T, Zwiers FW (2014) Consistency of temperature and precipitation extremes across various global gridded in situ and reanalysis datasets. *J Clim* 27:5019–5035. <https://doi.org/10.1775/JCLI-D-13-00405.1>
- Dyrødal AV, Isaksen K, Hygen HO, Meyer NK (2012) Changes in meteorological variables that can trigger natural hazards in Norway. *Clim Res* 55:153–165. <https://doi.org/10.3354/cr01125>
- Dyrødal AV, Skaugen T, Stordal F, Førland EJ (2016) Estimating extreme areal precipitation in Norway from a gridded dataset. *Hydrol Sci J* 61:483–494. <https://doi.org/10.1080/02626667.2014.947289>
- Førland EJ, Benestad RE, Flatoy F, Hanssen-Bauer I, Haugen JE, Isaksen K, Sorteberg A, Ådlandsvik B (2009) Climate development in north Norway and the Svalbard region during 1900–2100. Rapportserie 128, Norsk Polarinstittutt, 44 pp
- Frich P, Alexander LV, Della-Marta P, Gleason B, Haylock M, Klein Tank AMG, Peterson T (2002) Observed coherent changes in climatic extremes during the second half of the twentieth century. *Clim Res* 19:193–212. <https://doi.org/10.3354/cr019193>
- Giorgi F, Torma C, Coppola E, Ban N, Schär C, Somot S (2016) Enhanced summer convective rainfall at Alpine high elevations in response to climate warming. *Nat Geosci* 9:584–590. <https://doi.org/10.1038/NNGEO2761>
- Groisman PY, Knight RW, Easterling DR, Karl TR, Hegerl GC, Razuvayev VN (2005) Trends in intense precipitation in the climate record. *J Clim* 18:1326–1350. <https://doi.org/10.1175/JCLI3339.1>
- Groisman PY, Bogdanova EG, Alexeev VA, Cherry JE, Bulygina ON (2014) Impact of snowfall measurement deficiencies on quantification of precipitation and its trends over northern Eurasia. *Ice Snow* 2:29–43. <https://doi.org/10.15356/2076-6734-2014-2-29-43>
- Hansen BB et al (2014) Warmer and wetter winters: characteristics and implications of an extreme weather event in the high Arctic. *Environ Res Lett* 9:114021. <https://doi.org/10.1088/1748-9326/9/11/114021>
- Hanssen-Bauer I et al (2017) Climate in Norway 2100 – a knowledge base for climate adaption. Norwegian Centre for Climate Sciences, Oslo, p 48
- Hawcroft M, Walsh E, Hodges K, Zappa G (2018) Significantly increased extreme precipitation expected in Europe and North America from extratropical cyclones. *Environ Res Lett* 13:124006. <https://doi.org/10.1088/1748-9326/aaed59>

- Hellström C (2005) Atmospheric conditions during extreme and non-extreme precipitation events in Sweden. *Int J Climatol* 25:631–648. <https://doi.org/10.1002/joc.1119>
- Hellström C, Malmgren BA (2004) Spatial analysis of extreme precipitation in Sweden 1961–2000. *Ambio* 33: 187–192
- Hurrell JW, Kushnir Y, Ottersen G, Visbeck M (2003) An overview of the North Atlantic oscillation. In: Hurrell JW, Kushnir Y, Ottersen G, Visbeck M (eds) *The North Atlantic Oscillation: climatic significance and environmental impact*, vol 134. Geophysical Monograph Series, American Geophysical Union, Washington DC, pp 1–37
- Ionita M (2014) The impact of the East Atlantic/Western Russia pattern on the hydroclimatology of Europe from mid-winter to late spring. *Climate* 2:296–309. <https://doi.org/10.3390/cli2040296>
- Irannezhad M, Chen D, Kløve B (2016) The role of atmospheric circulation patterns in agroclimate variability in Finland: 1961–2011. *Geogr Ann* 98:287–301. <https://doi.org/10.1111/geoa.12137>
- Irannezhad M, Chen D, Kløve B, Moradkhani H (2017) Analysing the variability and trends of precipitation extremes in Finland and their connection to atmospheric circulation patterns. *Int J Climatol* 37:1053–1066. <https://doi.org/10.1002/joc.5059> (Corrigendum at <https://doi.org/10.1002/joc.6055>)
- Jaedicke C et al (2008) Spatial and temporal variations of Norwegian geohazards in a changing climate. *Nat Hazards Earth Syst Sci* 8:893–904. <https://doi.org/10.5194/nhess-8-893-2008>
- Jylhä K, Tuomenvirta H, Ruosteenoja K, Niemi-Hugaerts H, Keisu K, Karhu JA (2010) Observed and projected future shifts of climatic zones in Europe and their use to visualize climate change information. *Wea Clim Soc* 2:148–167. <https://doi.org/10.1175/2010WCAS1010.1>
- Kharin VV, Zwiers FW, Zhang X, Wehner M (2013) Changes in temperature and precipitation extremes in the CMIP5 ensemble. *Clim Chang* 119:345–357. <https://doi.org/10.1007/s10584-013-0705-8>
- Khlebnikova EI, Kattsov VM, Pikalova AA, Shkolnik IM (2018) Assessment of climate change impacts on the economic development of the Russian Arctic in the 21st century. *Russ Meteorol Hydrol* 43:347–356. <https://doi.org/10.3103/S1068373918060018>
- King AD, Karoly DJ (2017) Climate extremes in Europe at 1.5 and 2 degrees of global warming. *Environ Res Lett* 12:114031. <https://doi.org/10.1088/1748-9326/aa8e2c>
- Kivinen S, Rasmus S, Jylhä K, Laapas M (2017) Long-term climate trends and extreme events in northern Fennoscandia (1914–2013). *Clim* 5:16. <https://doi.org/10.3390/cli5010016>
- Klein Tank AMG, Können GP (2003) Trends in indices of daily temperature and precipitation extremes in Europe. *J Clim* 16:3665–3680. [https://doi.org/10.1175/1520-0442\(2003\)016<3665:TIOODT>2.0.CO;2](https://doi.org/10.1175/1520-0442(2003)016<3665:TIOODT>2.0.CO;2)
- Kochendorfer J et al (2017) The quantification and correction of wind-induced precipitation measurement errors. *Hydrol Earth Syst Sci* 21:1973–1989. <https://doi.org/10.5194/hess-21-1973-2017>
- Kopec BG, Feng X, Michel FA, Posmentier ES (2016) Influence of sea ice on Arctic precipitation. *Proc Natl Acad Sci* 113:46–51. <https://doi.org/10.1073/pnas.1504633113>
- Lamarre V, Legagneux P, Franke A, Casajus N, Currie DC, Berteaux D, Bêty J (2018) Precipitation and ectoparasitism reduce reproductive success in an arctic-nesting top-predator. *Sci Rep* 8:8530. <https://doi.org/10.1038/s41598-018-26131-y>
- Lehtonen I, Ruosteenoja K, Jylhä K (2014) Projected changes in European extreme precipitation indices on the basis of global and regional climate model ensembles. *Int J Climatol* 34:1208–1222. <https://doi.org/10.1002/joc.3758>
- Lim Y-K (2015) The East Atlantic/West Russia (EA/WR) teleconnection in the North Atlantic: climate impact and relation to Rossby wave propagation. *Clim Dyn* 44:3211–3222. <https://doi.org/10.1007/s00382-014-2381-4>
- Liu Y, Wang L, Zhou W, Chen W (2014) Three Eurasian teleconnection patterns: spatial structures, temporal variability, and associated winter climate anomalies. *Clim Dyn* 42:2817–2839. <https://doi.org/10.1007/s00382-014-2163-z>
- Luomaranta A, Aalto J, Jylhä K (2019) Snow cover trends in Finland over 1961–2004 based on gridded snow depth observations. *Int J Climatol* 39:3147–3159. <https://doi.org/10.1002/joc.6007>
- Lupikasza EB (2017) Seasonal patterns and consistency of extreme precipitation trends in Europe, December 1950 to February 2008. *Clim Res* 72:217–237. <https://doi.org/10.3354/cr01467>
- Marshall GJ, Vignols RM, Rees WG (2016) Climate change in the Kola Peninsula, Arctic Russia, during the last 50 years from meteorological observations. *J Clim* 29:6823–6840. <https://doi.org/10.1175/JCLI-D-16-0179.1>
- Marshall GJ, Kivinen S, Jylhä K, Vignols RM, Rees WG (2018) The accuracy of climate variability and trends across Arctic Fennoscandia in four reanalyses. *Int J Climatol* 38:3878–3895. <https://doi.org/10.1002/joc.5541>
- Mateeva TA, Gushchina DY, Zolina OG (2015) Large-scale indicators of extreme precipitation in coastal natural-economic zones of the European part of Russia. *Russ Meteorol Hydrol* 40:722–730. <https://doi.org/10.3103/S1068373915110023>

- Mestre O et al (2013) HOMER: a homogenization software – methods and applications. *Időjárás* 117:47–67
- Min S-K, Zhang X, Zwiers F (2008) Human-induced Arctic moistening. *Science* 320:518–520. <https://doi.org/10.1126/science.1153468>
- Moberg A et al (2006) Indices for daily temperature and precipitation extremes in Europe analyzed for the period 1901–2000. *J Geophys Res* 111:D22106. <https://doi.org/10.1029/2006JD007103>
- Nilsson C, Polvi LE, Lind L (2015) Extreme events in streams and rivers in arctic and subarctic regions in an uncertain future. *Freshw Biol* 60:2535–2546. <https://doi.org/10.1111/fwb.12477>
- O’Gorman PA (2014) Contrasting responses of mean and extreme snowfall to climate change. *Nature* 512:416–418. <https://doi.org/10.1038/nature13625>
- O’Gorman PA (2015) Precipitation extremes under climate change. *Curr Clim Change Rep* 1:49–59. <https://doi.org/10.1007/s40641-015-0009-3>
- Olsson T, Perttula T, Jylhä K, Luomaranta A (2017) Intense sea-effect snowfall case on the western coast of Finland. *Adv Sci Res* 14:231–239. <https://doi.org/10.5194/asr-14-231-2017>
- Overland JE et al (2016) Nonlinear response of mid-latitude weather to the changing Arctic. *Nat Clim Chang* 6:992–999. <https://doi.org/10.1038/NCLIMATE3121>
- Popova V (2007) Winter snow depth variability over northern Eurasia in relation to recent atmospheric circulation changes. *Int J Climatol* 27:1721–1733. <https://doi.org/10.1002/joc.1489>
- Räisänen J (2016) Twenty-first century changes in snowfall climate in Northern Europe in ENSEMBLES regional climate models. *Clim Dyn* 46:339–353. <https://doi.org/10.1007/s00382-015-2587-0>
- Reichstein M et al (2013) Climate extremes and the carbon cycle. *Nature* 500:287–295. <https://doi.org/10.1038/nature12350>
- Saha SK, Rinke A, Dethloff K (2006) Future winter extreme temperature and precipitation events in the Arctic. *Geophys Res Lett* 33:L15818. <https://doi.org/10.1029/2006GL026451>
- Sandvik MI, Sorteberg A, Rasmussen R (2018) Sensitivity of historically enhanced extreme precipitation events to idealized temperature perturbations. *Clim Dyn* 50:143–115. <https://doi.org/10.1007/s00382-017-3593-1>
- Scaife AA, Folland CK, Alexander LV, Moberg A, Knight JR (2008) European climate extremes and the North Atlantic Oscillation. *J Clim* 21:72–83. <https://doi.org/10.1175/2007JCLI1631.1>
- Schemm S, Sprenger M, Martius O, Wernli H, Zimmer M (2017) Increase in the number of extremely strong fronts over Europe? A study based on ERA-Interim reanalysis (1979–2014). *Geophys Res Lett* 44:553–561. <https://doi.org/10.1002/2016GL071451>
- Screen JA, Deser C, Sun L (2015) Projected changes in regional climate extremes arising from Arctic Sea ice loss. *Environ Res Lett* 10:084006. <https://doi.org/10.1088/1748-9326/10/8/084006>
- Sen PK (1968) Estimates of the regression coefficient based on Kendall’s tau. *J Am Stat Assoc* 63:1379–1389
- Sillmann J, Kharin VV, Zwiers FW, Zhang X, Bronaugh D (2013) Climate extreme indices in the CMIP5 multimodel ensemble: part 2. Future climate projections. *J Geophys Res Atmos* 118:2473–2493. <https://doi.org/10.1002/jgrd.50188>
- Tabari H, Willems P (2018) Lagged influence of Atlantic and Pacific climate patterns on European extreme precipitation. *Sci Rep* 8:5748. <https://doi.org/10.1038/s41598-018-24069-9>
- Taylor KE, Stouffer RJ, Meehl GA (2012) An overview of CMIP5 and the experiment design. *Bull Amer Meteor Soc* 93:485–498. <https://doi.org/10.1175/BAMS-D-11-00094.1>
- Vormoor K, Lawrence D, Schlichting L, Wilson D, Wong WK (2016) Evidence for changes in the magnitude and frequency of observed rainfall vs. snowmelt driven floods in Norway. *J Hydrol* 538:33–48. <https://doi.org/10.1016/j.hydrol.2016.03.066>
- Willems P (2013) Multidecadal oscillatory behaviour of rainfall extremes in Europe. *Clim Chang* 120:931–934. <https://doi.org/10.1007/s10584-013-0837-x>
- Yannic G, Aebischer A, Sabard B, Gilg O (2014) Complete breeding failures in ivory gull following unusual rainy storms in North Greenland. *Polar Res* 33:22749. <https://doi.org/10.3402/polar.v33.22749>
- Ye H (2018) Changes in duration of dry and wet spells associated with air temperatures in Russia. *Environ Res Lett* 13:034036. <https://doi.org/10.1088/1748-9326/aaae0d>
- Zhang X, Alexander L, Hegerl GC, Jones P, Klein Tank A, Peterson TC, Trewin B, Zwiers FW (2011) Indices for monitoring changes in extremes based on daily temperature and precipitation data. *WIREs Clim Change*. <https://doi.org/10.1002/wcc.147>
- Zolina O, Simmer C, Gulev SK, Kollet S (2010) Changing structure of European precipitation: longer wet periods leading to more abundant rainfalls. *Geophys Res Lett* 37:L06704. <https://doi.org/10.1029/2010GL042468>
- Zolina O, Simmer C, Belyaev K, Gulev SK, Koltermann P (2013) Changes in the duration of European wet and dry spells during the last 60 years. *J Clim* 26:2022–2047. <https://doi.org/10.1175/JCLI-D-11-00498.1>
- Zolotokrylin AN, Vinogradova VV, Titkova TB, Cherenkova EA, Bokuchava DD, Sokolov IA, Vinogradov AV, Babina ED (2018) Impact of climate changes on population vital activities in Russia in the early 21st century. *IOP Conf Ser: Earth and Environ Sci* 107:012045. <https://doi.org/10.1088/1755-1315/107/1/012045>

Zwart JA, Sebestyen SD, Solomon CT, Jones SE (2017) The influence of hydrologic residence time on lake carbon cycling dynamics following extreme precipitation events. *Ecosystems* 20:1000–1014. <https://doi.org/10.1007/s10021-016-0088-6>

Publisher's note Springer Nature remains neutral with regard to jurisdictional claims in published maps and institutional affiliations.

Affiliations

Gareth J. Marshall¹ · Kirsti Jylhä² · Sonja Kivinen³ · Mikko Laapas² · Anita Verpe Dyrrdal⁴

¹ British Antarctic Survey, Natural Environment Research Council, Cambridge, UK

² Weather and Climate Change Impact Research, Finnish Meteorological Institute, Helsinki, Finland

³ Department of Geographical and Historical Studies, University of Eastern Finland, Joensuu, Finland

⁴ Department of Model and Climate Analysis, Norwegian Meteorological Institute, Oslo, Norway